Dentomaxillofacial Radiology (2013) 42, 20120271

http://dmfr.birjournals.org

RESEARCH

Influence of dental materials on dental MRI

O Tymofiyeva*[,1], S Vaegler[1], K Rottner[2], J Boldt[2], AJ Hopfgartner[1], PC Proff[3], E-J Richter[2] and PM Jakob[1,4]

[1]*Department of Radiology and Biomedical Imaging, University of California, San Francisco, San Francisco, CA, USA;* [2]*Department of Prosthodontics, Dental School, University of Würzburg, Würzburg, Germany;* [3]*Department of Orthodontics, Dental School, University of Regensburg, Regensburg, Germany;* [4]*Magnetic Resonance Bavaria e.V., Würzburg, Germany*

Objectives: To investigate the potential influence of standard dental materials on dental MRI (dMRI) by estimating the magnetic susceptibility with the help of the MRI-based geometric distortion method and to classify the materials from the standpoint of dMRI.
Methods: A series of standard dental materials was studied on a 1.5 T MRI system using spin echo and gradient echo pulse sequences and their magnetic susceptibility was estimated using the geometric method. Measurements on samples of dental materials were supported by *in vivo* examples obtained in dedicated dMRI procedures.
Results: The tested materials showed a range of distortion degrees. The following materials were classified as fully *compatible* materials that can be present even in the tooth of interest: the resin-based sealer AH Plus® (Dentsply, Maillefer, Germany), glass ionomer cement, gutta-percha, zirconium dioxide and composites from one of the tested manufacturers. Interestingly, composites provided by the other manufacturer caused relatively strong distortions and were therefore classified as compatible I, along with amalgam, gold alloy, gold–ceramic crowns, titanium alloy and NiTi orthodontic wires. Materials, the magnetic susceptibility of which differed from that of water by more than 200 ppm, were classified as *non-compatible* materials that should not be present in the patient's mouth for any dMRI applications. They included stainless steel orthodontic appliances and CoCr.
Conclusions: A classification of the materials that complies with the standard grouping of materials according to their magnetic susceptibility was proposed and adopted for the purposes of dMRI. The proposed classification can serve as a guideline in future dMRI research.
Dentomaxillofacial Radiology (2013) **42,** 20120271. doi: 10.1259/dmfr.20120271

Cite this article as: Tymofiyeva O, Vaegler S, Rottner K, Boldt J, Hopfgartner AJ, Proff PC, et al. Influence of dental materials on dental MRI. *Dentomaxillofac Radiol* 2013; **42:** 20120271.

Keywords: Magnetic Resonance Imaging; Dental materials

Introduction

Recently, new approaches to the application of MRI in various branches of dentistry have been proposed in endodontics,[1] prosthodontics,[2,3] orthodontics[4] and diagnosis of dental caries.[5–7] However, dental materials present in the subject's mouth pose a major concern for dental applications of MRI. Magnetic susceptibility information is not readily available for many materials used in dentistry, especially those containing several components. Partly contradictory results have been reported regarding the severity of image artefacts caused by different dental materials.[8–17] For example, in some studies, high gold-content alloys were reported not to show any disturbance in phantoms[11,13] and porcine jaw *ex vivo*[12] but produced significant artefacts in other studies.[8,9] Similar contradictory results have been reported for titanium, dental amalgam and other materials. The strength of artefacts depends on many factors including magnetic field strength, pulse sequence, echo time, image resolution and the related gradient field strength, imaging plane, amount and shape of the dental material and distance between the object of interest and the material.[18] The conclusion about whether materials cause strong artefacts, moderate

*Correspondence to: Olga Tymofiyeva, Department of Radiology and Biomedical Imaging, University of California, San Francisco, San Francisco, CA, USA. E-mail: Olga.Tymofiyeva@ucsf.edu
Received 30 July 2012; revised 1 October 2012; accepted 31 October 2012

artefacts or no effect strongly depends on the specific application. For example, a material that is compatible with brain MRI can severely affect the quality of orofacial MRI. In contrast to the previous studies, a recent study on magnetic susceptibility and electric conductivity of metallic dental materials by Starcuková et al[17] considers this aspect. However, the variety of potential applications of MRI in dentistry requires a closer look at the MRI compatibility of dental materials.

In the case of conducting dental materials, there are wo potential sources of artefacts in MRI. The first source is the eddy currents induced by alternating gradients[19] and radiofrequency (RF) magnetic fields.[20] The induced eddy currents distort the applied RF field B_1 and this modifies the flip angle, leading to image distortion. The second source is distortion of the static magnetic field B_0 due to the difference in magnetic susceptibilities of materials and body tissues. In most cases, B_0 effects are predominant[21] and this study concentrates on them.

Body tissues are weakly diamagnetic and have a magnetic susceptibility, χ, close to that of water, $\chi_{water} = -9.05 \times 10^{-6}$.[18] Susceptibility differences between imaged substances affect the homogeneity of the magnetic field in the imaged volume and cause image distortions in MRI experiments. Susceptibility artefacts appear in gradient echo (GE)-based images as loss of signal around the material due to dephasing within a pixel or a slice, and in spin echo (SE)-based images as complex spear-shaped artefacts resulting from slice selection and position-encoding distortions. In general, use of SE-based, instead of GE-based, pulse sequences reduces susceptibility artefacts. Since there is no refocusing 180° pulse, T_2* effects are not reversed in GE-based techniques, resulting in a greater dephasing of spins than in SE-based techniques. The new techniques for direct imaging of hard tissues[6,7] are relatively insensitive to magnetic susceptibility artefacts owing to the short delay between excitation and acquisition. Additionally, specially designed sequences such as multiacquisition with variable resonance image combination[22] and slice-encoding metal artefact correction[23] significantly reduce the size and intensity of susceptibility artefacts. However, the use of conventional pulse sequences prevails.

Although the magnetic susceptibility values of many materials are unavailable, they can be estimated from the caused distortions in an MR image, for example, using the geometric MRI method.[24] There are two special cases of sample geometry for which an analytical solution for the internal and external field exists: spheres and cylinders.[18,25] For example, a cylinder with a radius of R oriented transversely to the main magnetic field B_0 causes a distortion L_z in the frequency-encoding direction in SE images. The susceptibility difference between the cylinder material and the surrounding medium can be derived as:[21,24]

$$\Delta\chi = 2G_r L_z^3 / (B_0 k_z^3 R^2) \quad (1)$$

where G_r is the gradient strength and k_z is a dimensionless geometry-related parameter, $k_z \approx 2.828986$.

The geometric method was shown to be suitable for quick estimations of susceptibility values[24] and reliable for Al, Ti and other materials with a bad susceptibility match.[21]

The purpose of this study was (i) to investigate the potential influence of standard dental materials on dental MRI (dMRI) by estimating the magnetic susceptibility with the help of the MRI-based geometric method and (ii) to classify the materials from the standpoint of dMRI.

Materials and methods

In vitro *measurements*

There are four classes of dental materials:[26] metals, ceramics, polymers and composites. A series of standard dental materials from different classes listed in Table 1 was studied on a 1.5 T MRI system (Magnetom® Avanto; Siemens Medical Solutions, Erlangen, Germany) using a 4 cm diameter RF surface coil. Materials were placed on poly-ether–ether–ketone (PEEK; $\chi_{PEEK} = -9.3 \times 10^{-6}$)[27] cylinders and immersed in water doped with 0.15% Magnevist® (Schering AG, Berlin, Germany) to reduce the measurement time. The cylinders were oriented perpendicular to the static magnetic field B_0. SE and GE images were acquired. The measurement parameters of the three-dimensional (3D) turbo-spin echo (TSE) sequence were: repetition time (TR)/echo time (TE), 400 ms/14 ms; turbo factor (TF), 5; field of view (FOV), $49 \times 49 \times 10.8$ mm^3; matrix, $128 \times 128 \times 30$; bandwidth, 130 Hz per pixel. The measurement parameters of the 3D GE sequence were: TR/TE, 18 ms/9.5 ms; α, 40°; FOV, $120 \times 120 \times 30.2$ mm^3; matrix, $320 \times 320 \times 72$; bandwidth, 190 Hz per pixel. Image distortions were analysed for cylindrically shaped materials by measuring the length L_z in the SE images (Figure 1) and the magnetic susceptibility was estimated according to Equation (1).

Based on the classification proposed in the comprehensive review article on the role of magnetic susceptibility in MRI by Schenck,[18] the materials were divided into three groups according to the susceptibility difference, $\Delta\chi = \chi_{material} - \chi_{water}$, as follows:

Compatible: $|\Delta\chi| < 3$ ppm, the material produces no detectable distortions on either SE or GE imaging

Compatible I: $3 < |\Delta\chi| < 200$ ppm, the material produces noticeable distortions, acceptance depends on the application

Non-compatible: $|\Delta\chi| > 200$ ppm, the material produces strong image distortions even when it is located far from the imaging region.

This classification also serves as a definition of "detectable", "noticeable" and "strong" image distortions by relating the distortion length L_z to the actual radius R of the cylindrically shaped material through Equation (1).

Since, in the first series of measurements, the composite material that was not expected to produce artefacts

Table 1 Dental MRI compatibility of dental materials at 1.5 T. Compatible: $|\Delta\chi| < 3$ ppm, the material can be present in the tooth of interest; compatible I: $3 < |\Delta\chi| < 200$ ppm, the material should not be present in the tooth of interest or its neighbours or antagonists; non-compatible: $|\Delta\chi| > 200$ ppm, the material should not be present in the mouth

Material	*Function and composition*	*Manufacturer*	*dMRI compatibility*
AH Plus resin	Two-component paste/paste root canal sealer based on epoxy-amine resin	Dentsply (Maillefer, Germany)	Compatible
Amalgam	Dental restorative material consisting of about 50% liquid mercury by weight and 20–35% powdered silver, with the remainder comprising tin, copper, zinc and other metals	Degussa (Frankfurt, Germany)	Compatible I
CoCr	Alloy with the appoximate composition of 60% Co, 25% Cr, 10% Ni, 5% Mo and 0.3% C used in both orthodontics and prosthetic dentistry	Amann Girrbach (Koblach, Austria)	Non-compatible
Composites	Synthetic resins composed of a soft organic matrix and hard inorganic fillers (silica) cured by photopolymerization and used as restorative material or adhesives; inorganic oxides and organic compounds (most commonly, iron oxides) are added as pigments to create a range of various composite shades	3M ESPE (Seefeld, Germany) – Filtek Supreme XT Universal, Filtek Supreme XT Flowable, Filtek Z250, Filtek P60 Posterior Restorative, shades A3, B3, C3	Compatible
		Ivoclar Vivadent (Ellwangen, Germany) – Tetric Ceram and Tetric Flow, shades A1–A4, B3, C3, D3, transparent, bleach	Compatible I
Glass ionomer cement	Dental restorative material based on the reaction of silicate glass powder and polyalkenoic acid used for filling teeth and luting cements	3M ESPE	Compatible
Gold alloy	The oldest dental restorative material, containing, for example, 85.6% gold, 12.7% platinum, 0.2% iridium, 0.1% rhodium and traces of indium, zinc, titanium, iron	DeguDent (Hanau, Germany)	Compatible I
Gold–ceramic crown	Porcelain-fused-to-metal crown with the use of a gold alloy	DeguDent	Compatible I
Gutta-percha	Rubber-like coagulated juice of tropical trees used for temporary sealing of dressings in cavities and for filling root canals in endodontics	Demedi-Dent (Dortmund, Germany)	Compatible
Titanium alloy	Alloy with 6% Al and 4% V or in pure form used as a dental implant material	Friadent (Mannheim, Germany)	Compatible I
Zirconium dioxide	High strength and hardness ceramic material used for production of CAD/CAM restorations and implants	Metoxit (Thayngen, Switzerland)	Compatible
Orthodontic wires			
NiTi alloy wire	Used in orthodontics to maintain existing dental positions or to straighten teeth	Dentaurum (Ispringen, Germany)	Compatible I
Stainless steel wire		Dentaurum	Non-compatible
Stainless steel brackets		Dentaurum	Non-compatible

CAD, computer-aided design; CAM, computer-aided manufacturing.

showed noticeable distortions, the study was extended to include additional 24 composite materials from two manufacturers: 3M ESPE, Seefeld, Germany and Ivoclar Vivadent, Ellwangen, Germany (Table 1). The composite samples were shaped as cylinders of diameter $d = 5.400 \pm 0.025$ mm and suspended in a 1.5% agar solution. Only two-dimensional (2D) SE measurements were performed, with TR/TE, 670 ms/37 ms; FOV, 40×40 mm^2; matrix, 256×256; slice thickness, 0.7 mm; and bandwidth, 40 Hz per pixel. The distortions of the cylinder shape on the images were analysed and the magnetic susceptibility was estimated according to Equation (1).

In vivo *measurements*

To translate the effect of susceptibility mismatch to the *in vivo* situation and explicate the classification of the materials, dMRI of subjects who participated in earlier dMRI studies[2,4] and had different dental materials present in the mouth were analysed retrospectively. The materials included dental composites, gold–ceramic crowns, stainless steel and NiTi retainers, and stainless steel braces.

Apart from 2D GE-based scout scans, two kinds of 3D TSE dMRI acquisitions were analysed. The first kind provided a very high resolution for tooth surface digitization with the use of an oral Gd-based contrast medium and intraoral RF coil.[2] The measurement parameters were: TR/TE, 400 ms/12 ms; TF, 5; FOV, $60 \times 30 \times 17$mm^3; resolution, $0.3 \times 0.3 \times 0.3$ mm^3; bandwidth, 230 Hz per pixel; measurement time, 8 min. The second kind of measurements provided 3D data sets with a lower spatial resolution for orthodontic treatment and surgery planning.[4] Extraoral RF coils were utilized. No oral contrast medium was applied and the surface of the teeth was visualized owing to the contrast between the

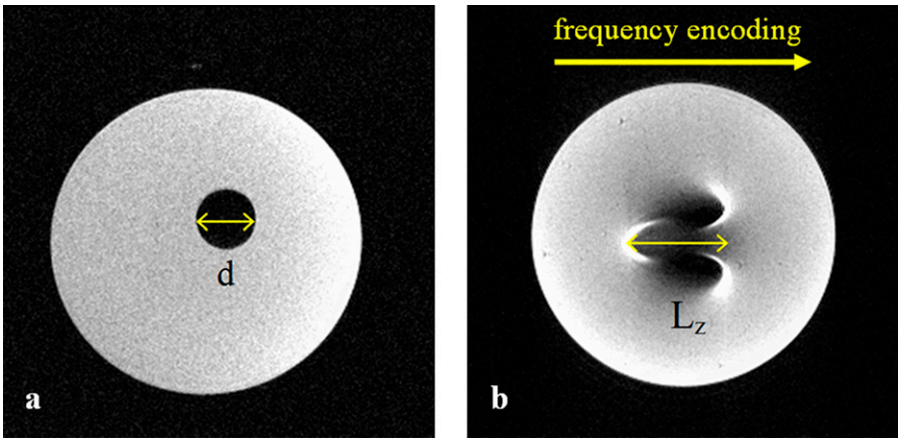

Figure 1 (a) Two-dimensional (2D) spin echo (SE) image of a compatible composite Filtek Supreme XT Flowable (3M ESPE, Seefeld, Germany). (b) 2D SE image of a compatible I composite Tetric Flow (Ivoclar Vivadent, Ellwangen, Germany)

teeth and surrounding soft tissues. The measurement parameters were: TR/TE, 1000ms/10 ms; TF, 17; FOV, $10 \times 6 \times 5\,cm^3$; resolution, $0.78 \times 0.78 \times 1\,mm^3$; bandwidth, 200 Hz per pixel; measurement time, 4–5 min.

All *in vivo* measurements were performed on a 1.5 T Magnetom Avanto MRI scanner. Tooth surface reconstruction was performed using Amira (ZIB, Berlin, Germany). The distortion of the tooth shape was analysed qualitatively by visual inspection of the differences between the reconstructed surface and the natural tooth shape supported by panoramic radiograph images.

Results

In vitro *measurements*

The tested materials showed a range of distortion degrees. The results of material classification are summarised in Table 1. Examples of SE and GE images of dental materials from the three different classes are shown in Figure 2.

The following materials were classified as fully compatible materials that can be present even in the tooth of interest: the resin-based sealer AH Plus, glass ionomer cement, gutta-percha, zirconium dioxide and some composites. The additional study of composite materials from different manufacturers showed an interesting result. None of the 3M ESPE composites studied caused any detectable distortions (Figure 1a), demonstrating a magnetic susceptibility close to that of the surrounding medium. All Ivoclar Vivadent composites studied caused significant artefacts (Figures 1b and 2). From the direction of the distortion, it could be concluded that the materials are paramagnetic. The susceptibility magnitude estimated based on the distortion L_z (Figure 1b) according to Equation (1) was in the range of $(17.0 \pm 4.5) \times 10^{-6}$ to $(35.0 \pm 6.5) \times 10^{-6}$, and thus the difference to the susceptibility of water was $3 < |\Delta\chi| < 200$ ppm. Based on this result, Ivoclar Vivadent composites were classified as compatible I, along with amalgam, gold alloy, gold–ceramic crowns, titanium alloy and NiTi orthodontic wires.

Finally, the stainless steel orthodontic appliances and CoCr sample showed the strongest distortions and were classified as non-compatible.

In vivo *measurements*

An *in vivo* example of using a compatible composite (3M ESPE) in a tooth prepared for an inlay is shown in Figure 3a. The non-distorted tooth surface reconstruction obtained using the high-resolution contrast-enhanced dMRI *in vivo* procedure is shown in Figure 3b.

As mentioned above, relatively strong distortions (compatible I) were caused by some composite materials, an *in vivo* example of which is shown in Figure 4. Amalgam and gold alloys were also characterized as compatible I, leading to noticeable distortions of the reconstructed tooth surface (Figure 5).

In vivo examples of a stainless steel retainer and braces are shown in Figure 6a,b. NiTi wires caused smaller artefacts (compatible I), in which 3D reconstructions became apparent as slight distortions of the tooth surface (Figure 7).

Discussion

Development of MRI applications in dentistry sets new requirements for the compatibility of dental materials. Although solutions for artefact correction are being sought, foreign materials in the body remain an issue. The influence of dental materials on MRI in general has been studied previously. However, dental applications of MRI are more susceptible to the presence of dental materials. In the presented study, a series of standard dental materials was studied on a 1.5 T MRI system using SE and GE pulse sequences and image distortions were analysed from the standpoint of dMRI. The observed artefacts could be, with a high probability, attributed to susceptibility artefacts and not to eddy currents. However, although in

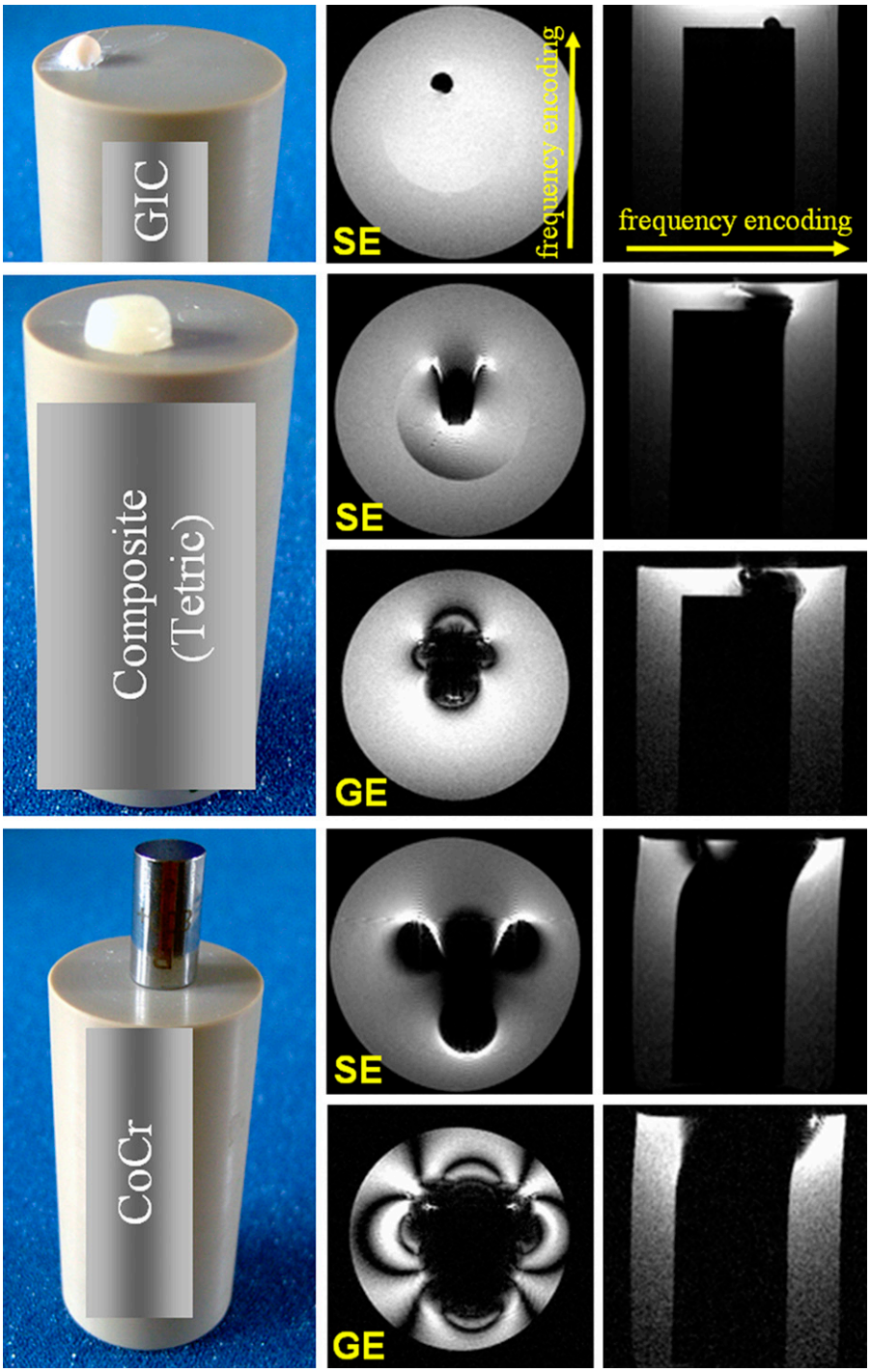

Figure 2 Photographs and spin echo (SE) and gradient echo (GE) images of glass ionomer cement (GIC), composite and CoCr samples. Two measurements were performed: one with the slab oriented transverse and one parallel to the poly-ether–ether–ketone cylinder axis

most cases B_0 effects are predominant, flip angle modification due to induced eddy currents can play a dominant role in the case of conducting materials with a small magnetic susceptibility mismatch. Thus, bright spots observed in the vicinity of a precious metal alloy crown can be induced by eddy currents.[16]

The analysis of the obtained *in vitro* results allowed for the classification of materials based on the magnetic susceptibility for the purposes of dMRI. Table 1 specifies that materials that belong to the group compatible can be present in the tooth of interest, even if a very precise reconstruction of the tooth surface is required, *e.g.* a digital dental impression for production of dental restorations using CAD/CAM technology.[2,3] An *in vivo* example of using a compatible composite restorative material in a tooth prepared for an inlay is shown in Figure 3.

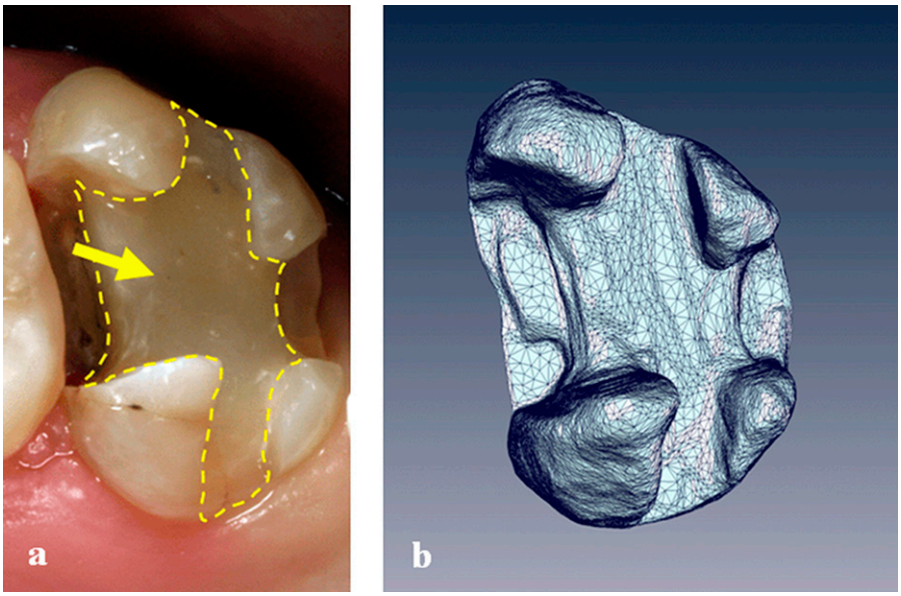

Figure 3 (a) Tooth built up using a 3M ESPE (Seefeld, Germany) composite and prepared for an inlay. (b) Three-dimensional (3D) reconstruction of the tooth surface based on an *in vivo* dental MRI measurement

Materials from the group compatible I should be used with care if dMRI is considered. Such materials should not be present in the tooth of interest or its neighbours or antagonists if a true representation of the tooth surface is required. In the case of dMRI applications with lower requirements for the precision of the reconstructed tooth surface, such as orthodontic treatment planning, the presence of materials from the group compatible I is not critical (Figures 4, 5, 7).

This study provides a new piece of information about composite dental materials. Whereas composites of some manufacturers had an almost perfect susceptibility match to water and were therefore compatible for dMRI, others showed markedly paramagnetic properties and caused significant distortions. The paramagnetic properties can possibly be explained by iron oxide pigments often used by manufacturers. The smallest contamination by ferromagnetic substances can drastically alter the susceptibility of a magnetically compatible material.[18] For example, Schenck[18] noticed that ceramic silicon nitride provided by some vendors had an almost perfect susceptibility match to water, while that from other vendors was markedly paramagnetic, probably as a result of minute quantities of iron oxide incorporated in the binding material. Another example describes surface contamination of a copper rod by iron or steel particles introduced during the manufacturing process. Interestingly, the iron atoms in deoxyhaemoglobin give rise to the susceptibility difference between deoxygenated blood and surrounding tissue, which forms the basis of functional MRI.[18] However, in the context of our study, susceptibility differences caused by iron clearly pose a problem. One can assume that different quantities of the pigment are required to create different shades of dental composites. Our study, however, showed no correlation between the measured distortions and the material shade. In the case of high-resolution dMRI applications, such as diagnosis of caries or MRI-based dental impressions, it is of paramount importance to use compatible composite materials in the tooth of interest or its neighbours or antagonists. The smallest distortion, in the range of hundreds of micrometres, of the reconstructed tooth surface, cavity in the tooth or dental pulp is critical and can make the results of the measurement useless.

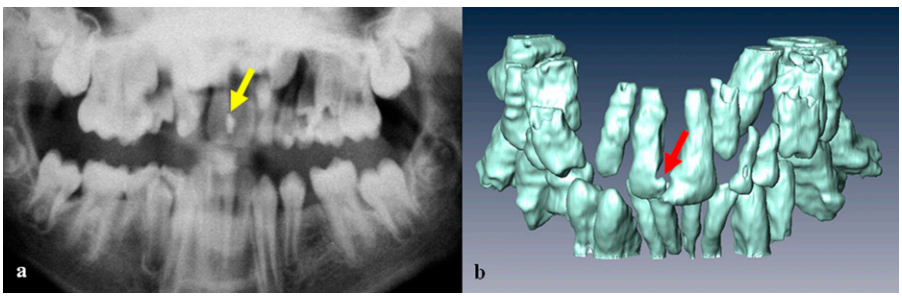

Figure 4 Panoramic radiograph image (a) and a three-dimensional MRI reconstruction (b) of the teeth of a volunteer with a compatible I composite filling in the maxillary central incisors (arrows)

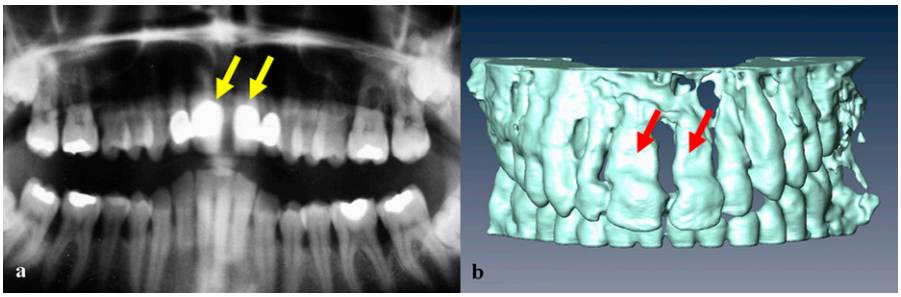

Figure 5 Panoramic radiograph image (a) and a three-dimensional MRI reconstruction (b) of the teeth of a volunteer with gold–ceramic crowns in the maxillary incisors (arrows)

The third group, non-compatible, contains materials posing the highest difficulty for dMRI. Highly paramagnetic materials, such as stainless steel or CoCr, cause loss of signal around the material owing to dephasing within a pixel or a slice in GE-based images, and complex spear-shaped artefacts in SE-based images, for which slice selection and position-encoding distortions are responsible. Materials belonging to this group should not be present in the mouth if a dMRI measurement is considered.

In practice, major problems are expected in the case of fixed metallic orthodontic appliances such as stainless steel retainers. When well fixed, retainers pose no risk to the patient in the magnetic field of a clinical MRI scanner;[28] however, imaging quality suffers significantly. A better choice from the standpoint of dMRI is nickel–titanium alloys[18] as demonstrated in Figure 7. The local distortions caused by a nickel–titanium alloy that are shown in Figure 7b would not affect the diagnostic value of MR images acquired for orthodontic purposes.

It should be noted that the equation used for estimating the susceptibility difference, Equation (1), was introduced for basic 2D SE sequences. In our study, we partly applied this approach to 3D TSE sequences. In 3D sequences, a second phase encoding is performed in the slab direction. However, since the susceptibility difference-induced field component interferes only with the frequency-encoding process, it distorts the image in the readout but not in the phase-encoding direction.[18] Another deviation we made was the use of turbo (fast) SE sequences. It has been reported in previous studies, for example, that T_2 weighted TSE sequences appreciably reduce susceptibility artefacts when compared with T_2 weighted SE sequences.[29] The authors explained this reduction by the difference in the TE and/or echo spacing between TSE and conventional SE imaging. They state that "the period of time between the 180° refocusing pulse and the echo at TE is considerably longer, allowing for increased dephasing of spins".[29] And since the true echo space in TSE sequences is considerably shorter than the effective TE, at which the contrast-determining central areas of the *k*-space are filled, there is a much more limited period of time between each 180° refocusing pulse for spins to dephase before each echo is measured. This, however, contradicts our understanding of the refocusing mechanism, according to which distortions in SE images do not increase as a function of time precisely because the 180° pulse refocuses spins that have been dephased by field inhomogeneities.[18] Another group reported that they "were surprised that decreasing TE did not reduce the mean artefact size for conventional spin-echo sequences",[30] which we find to be a plausible finding.

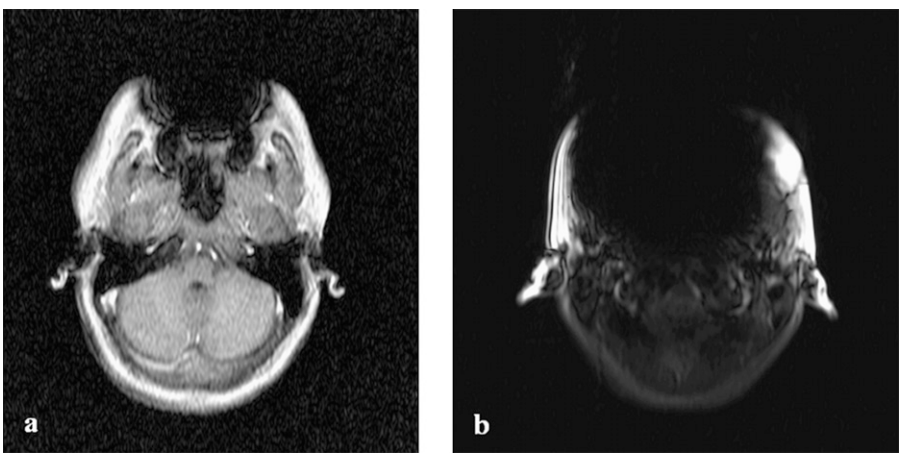

Figure 6 (a) MRI scout scan of a volunteer with a stainless steel retainer. Signal void is seen in the region of the teeth. (b) MRI scout scan of a volunteer with stainless steel braces on the lower arch

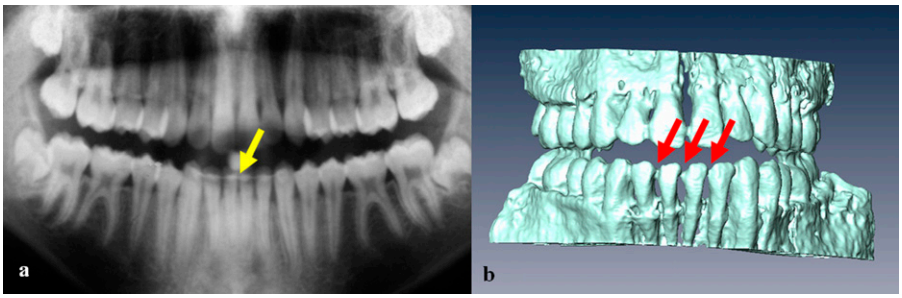

Figure 7 Panoramic radiograph image (a) and a three-dimensional MRI reconstruction (b) of the teeth of a volunteer with an NiTi retainer (arrows)

Unambiguous classification of dental materials according to MRI compatibility is only possible when it is based on constant material properties such as magnetic susceptibility. Otherwise, too many parameters have to be specified, which is usually impossible and leads to contradictory results. The classification proposed in this paper is based on the magnetic susceptibility of the materials and complies with the classification proposed in the review article on the role of magnetic susceptibility in MRI by Schenck.[18] Additionally, each group is described from the standpoint of dMRI applications and supported by *in vivo* examples obtained in dedicated dMRI procedures, which distinguishes the presented study from most previous publications on MRI compatibility of dental materials.

In conclusion, the proposed classification of dental materials can serve as a useful guideline in future dMRI research.

References

1. Kress B, Buhl Y, Anders L, Stippich C, Palm F, Bahren W, et al. Quantitative analysis of MRI signal intensity as a tool for evaluating tooth pulp vitality. *Dentomaxillofac Radiol* 2004; **33**: 241–244.
2. Tymofiyeva O, Rottner K, Gareis D, Boldt J, Schmid F, Lopez MA, et al. In vivo MRI-based dental impression using an intraoral RF receiver coil. *Concept Magn Reson B: Magn Reson Eng* 2008; **33B**: 244–251.
3. Tymofiyeva O, Schmid F, von Kienlin M, Breuer FA, Rottner K, Boldt J, et al. On precise localization of boundaries between extended uniform objects in MRI: tooth imaging as an example. *Magn Reson Mater Phys* 2011; **24**: 19–28.
4. Tymofiyeva O, Rottner K, Jakob PM, Richter E, Proff P. Three-dimensional localization of impacted teeth using magnetic resonance imaging. *Clin Oral Investig* 2010; **14**: 169–176.
5. Tymofiyeva O, Boldt J, Rottner K, Schmid F, Richter E-J, Jakob PM. High-resolution 3D magnetic resonance imaging and quantification of carious lesions and dental pulp in vivo. *MAGMA* 2009; **22**: 365–374.
6. Idiyatullin D, Corum C, Moeller S, Prasad HS, Garwood M, Nixdorf DR. Dental magnetic resonance imaging: making the invisible visible. *J Endod* 2011; **37**: 745–752.
7. Bracher A-K, Hofmann C, Bornstedt A, Boujraf S, Hell E, Ulrici J, et al. Feasibility of ultra-short echo time (UTE) magnetic resonance imaging for identification of carious lesions. *Magn Reson Med* 2011; **66**: 538–545.
8. Abbaszadeh K, Heffez LB, Mafee MF. Effect of interference of metallic objects on interpretation of T1-weighted magnetic resonance images in the maxillofacial region. *Oral Surg Oral Med Oral Pathol Oral Radiol Endod* 2000; **89**: 759–765.
9. Beuf O, Lissac M, Crémillieux Y, Briguet A. Correlation between magnetic resonance imaging disturbances and the magnetic susceptibility of dental materials. *Dent Mater* 1994; **10**: 265–268.
10. Costa AL, Appenzeller S, Yasuda CL, Pereira FR, Zanardi VA, Cendes F. Artifacts in brain magnetic resonance imaging due to metallic dental objects. *Med Oral Patol Oral Cir Bucal* 2009; **14**: E278–E282.
11. Destine D, Mizutani H, Igarashi Y. Metallic artifacts in MRI caused by dental alloys and magnetic keeper. *J Jpn Prosthodont Soc* 2008; **52**: 205–210.
12. Eggers G, Rieker M, Kress B, Fiebach J, Dickhaus H, Hassfeld S. Artefacts in magnetic resonance imaging caused by dental material. *MAGMA* 2005; **18**: 103–111.
13. Lissac M, Metrop D, Brugirard J, Coudert JL, Pimmel P, Briguet A, et al. Dental materials and magnetic resonance imaging. *Invest Radiol* 1991; **26**: 40–45.
14. Masumi S, Arita M, Morikawa M, Toyoda S. Effect of dental metals on magnetic resonance imaging (MRI). *J Oral Rehabil* 1993; **20**: 97–106.
15. Shafiei F, Honda E, Takahashi H, Sasaki T. Artifacts from dental casting alloys in magnetic resonance imaging. *J Dent Res* 2003; **82**: 602–606.
16. Starčuk Z, Bartušek K, Hubálková H, Bachorec T, Starčuková J, Krupa P. Evaluation of MRI artifacts caused by metallic dental implants and classification of the dental materials in use. *Meas Sci Rev* 2006; **6**: 24–27.
17. Starcuková J, Starcuk Z Jr, Hubálková H, Linetskiy I. Magnetic susceptibility and electrical conductivity of metallic dental materials and their impact on MR imaging artifacts. *Dent Mater* 2008; **24**: 715–723.
18. Schenck JF. The role of magnetic susceptibility in magnetic resonance imaging: MRI magnetic compatibility of the first and second kinds. *Med Phys* 1996; **23**: 815–850.
19. Camacho CR, Plewes DB, Henkelman RM. Nonsusceptibility artifacts due to metallic objects in MR imaging. *J Magn Reson Imaging* 1995; **5**: 75–88.
20. Graf H, Steidle G, Martirosian P, Lauer UA, Schick F. Metal artifacts caused by gradient switching. *Magn Reson Med* 2005; **54**: 231–234.
21. Koivula A. *Magnetic resonance image distortions due to artificial macroscopic objects. An example: correction of image distortion caused by an artificial hip prosthesis.* Dissertation. Oulu, Finland: University of Oulu; 2002.
22. Koch KM, Lorbiecki JE, Hinks RS, King KF. A multispectral three-dimensional acquisition technique for imaging near metal implants. *Magn Reson Med* 2009; **61**: 381–390.
23. Lu W, Pauly KB, Gold GE, Pauly JM, Hargreaves BA. SEMAC: slice encoding for metal artifact correction in MRI. *Magn Reson Med* 2009; **62**: 66–76.

24. Schenck JF. Quantitative analysis of intensity artifacts in spin-echo images produced by variations in magnetic susceptibility within the field of view: equations for the rapid determination of susceptibilities and analogies with catastrophe optics and optical caustic curves. In: Proceedings of the 12th Annual Meeting of the Society for Magnetic Resonance in Medicine (SMRM); 14–20 August, 1993; Berkeley, CA. Berkeley, CA: SMRM; 1993.
25. Lüdeke KM, Röschmann P, Tischler R. Susceptibility artefacts in NMR imaging. *Magn Reson Imaging* 1985; **3**: 329–343.
26. Ferracane JL. *Materials in dentistry*: principles and applications. Philadelphia, PA: Lippincott Williams & Wilkins; 2001.
27. Doty FD, Entzminger G, Yang YA. Magnetism in high-resolution NMR probe design. I. General methods. *Concepts Magn Reson A* 1998; **10**: 133–156.
28. Klocke A, Kahl-Nieke B, Adam G, Kemper J. Magnetic forces on orthodontic wires in high field magnetic resonance imaging (MRI) at 3 Tesla. *J Orofac Orthop* 2006; **67**: 424–429.
29. Tartaglino LM, Flanders AE, Vinitski S, Friedman DP. Metallic artifacts on MR images of the postoperative spine: reduction with fast spin-echo techniques. *Radiology* 1994; **190**: 565–569.
30. Petersilge CA, Lewin JS, Duerk JL, Yoo JU, Ghaneyem AJ. Optimizing imaging parameters for MR evaluation of the spine with titanium pedicle screws. *AJR Am J Roentgenol* 1996; **166**: 1213–1218.